# The EUMETSAT Satellite Application Facility on Land Surface Analysis (LSA SAF)

# Product User Manual

# Evapotranspiration (ET)

**PRODUCTS: LSA-301 (MET), LSA- 302 (DMET)**

The EUMETSAT Network of Satellite Application Facilities

LSA SAF Land Surface Analysis

| | |
|---|---|
| Reference Number: | SAF/LAND/IM/PUM_MET/2.4 |
| Issue/Revision Index: | Issue 2.5 |
| Last Change: | 25/11/2015 |

# DOCUMENT SIGNATURE TABLE

| | **Name** | **Date** | **Signature** |
|---|---|---|---|
| **Prepared by :** | RMI Team | 10/07/2008 | |
| **Approved by :** | Land SAF Project Manager (IPMA) | 10/07/2008 | |

# DOCUMENTATION CHANGE RECORD

| **Issue / Revision** | **Date** | **Description:** |
|---|---|---|
| Version 1.0 | 26/07/2007 | Version presented at Checkpoint Meeting (04/09 2007) |
| Version 2.0 | 11/04/2008 | Version presented for the ORR3 review (14 /05/2008) |
| Version 2.1 | 10/07/2008 | Improved version after ORR3 review |
| Version 2.2 | 12/03/2010 | Version provided for the ORR (14/4/2010); based on version 2.1 by including information on DMET. |
| Version 2.3 | 11/10/2010 | Version presented after ORR 04/2010 including incorporating answers to RIDS (in order to declare MET operational and DMET pro-operational). |
| Version 2.4 | 08/04/2011 | Version presented for OR-5 (April 2011), including comparison of daily ET to ground measurements. |
| Version 2.5 | 25/11/2015 | Change coverage area of MSG products<br>Change acronym IM -> IPMA<br>Update distribution list |
| | | |

# DISTRIBUTION LIST

| **Internal Consortium Distribution** | | |
|---|---|---|
| **Organisation** | **Name** | **No. Copies** |
| IPMA | Isabel Trigo | |
| | Sandra Coelho | |
| | Carla Sofia Barroso | |
| | Isabel Monteiro | |
| | Pedro Diegues | |
| | Pedro Ferreira | |
| | Ana Veloso | |
| | Ricardo Torres | |
| | Nuno Simões | |
| IDL | Carlos da Camara | |
| | Teresa Leal Rosa | |
| | Teresa Calado | |
| | Sofia Ermida | |
| M-F | Jean-Louis Roujean | |
| | Dominique Carrer | |
| | Gregoire Jacob | |
| RMI | Francoise Meulenberghs | |
| | Arboleda Alirio | |
| | Nicolas Ghilain | |
| KIT | Folke Olesen | |
| | Frank.Goettsche | |
| UV | Joaquin Melia | |
| | Fernando Camacho | |
| | Javier Garcia | |
| | Aleixandre Verger | |
| KCL | Martin Wooster | |
| | Jiangping He | |
| | Daniel Fisher | |
| | Weidong Xu | |
| VITO | Smets Bruno | |
| | Bydekerke Lieven | |

| **External Distribution** | | |
|---|---|---|
| **Organisation** | **Name** | **No. Copies** |
| EUMETSAT | Frédéric Gasiglia | |
| EUMETSAT | Dominique Faucher | |
| EUMETSAT | Lorenzo Sarlo | |
| EUMETSAT | Lothar Schueller | |
| EDISOFT | Joana Rosa | |
| EDISOFT | Joaquim Araújo | |
| JMV | Mauro Lima | |

| **Steering Group Distribution** | | |
|---|---|---|
| **Nominated by:** | **Name** | **No. Copies** |
| IPMA | Carlos Direitinho Tavares | |
| EUMETSAT | Lorenzo Sarlo | |
| EUMETSAT | Yves Govaerts | |
| EUMETSAT | François Montagner | |
| STG/AFG (USAM) | Luigi de Leonibus | |
| MF | François Bouyssel | |
| RMI | Steven Dewitte | |
| FMI | Carl Fortelius | |

# TABLE OF CONTENTS

# 1 Introduction

The Satellite Application Facility (SAF) on Land Surface Analysis (LSA) is part of the SAF Network, a set of specialised development and processing centres, serving as EUMETSAT (European organization for the Exploitation of Meteorological Satellites) distributed Applications Ground Segment. The SAF network complements the product-oriented activities at the EUMETSAT Central Facility in Darmstadt. The main purpose of the LSA SAF is to take full advantage of remotely sensed data, particularly those available from EUMETSAT sensors, to measure land surface variables, which will find primarily applications in meteorology (http://landsaf.ipma.pt/)

The spin-stabilised Meteosat Second Generation (MSG) has an imaging-repeat cycle of 15 minutes. The Spinning Enhanced Visible and Infrared Imager (SEVIRI) radiometer embarked on the MSG platform encompasses unique spectral characteristics and accuracy, with a 3 km resolution (sampling distance) at nadir (1km for the high-resolution visible channel), and 12 spectral channels (Schmetz et al., 2002).

The EUMETSAT Polar System (EPS) is Europe's first polar orbiting operational meteorological satellite and the European contribution to a joint polar system with the U.S. EUMETSAT will have the operational responsibility for the "morning orbit" with Meteorological-Operational (MetOp) satellites, the first of which was successfully launched on October 19, 2006. Despite the wide range of sensors on-board MetOp (http://www.eumetsat.int/), most LSA SAF parameters make use of the Advanced Very High Resolution Radiometer (AVHRR) and, to a lesser extent, of the Advanced Scatterometer (ASCAT).

Several studies have stressed the role of land surface processes on weather forecasting and climate modelling (e.g., Dickinson et al., 1983; Mitchell et al., 2004; Ferranti and Viterbo, 2006). The LSA SAF has been especially designed to serve the needs of the meteorological community, particularly Numerical Weather Prediction (NWP). However, there is no doubt that the LSA SAF addresses a much broader community, which includes users from:

- Weather forecasting and climate modelling, requiring detailed information on the nature and properties of land.
- Environmental management and land use, needing information on land cover type and land cover changes (e.g. provided by biophysical parameters or thermal characteristics).
- Agricultural and Forestry applications, requiring information on incoming/outgoing radiation and vegetation properties.
- Renewable energy resources assessment, particularly biomass, depending on biophysical parameters, and solar energy.
- Natural hazards management, requiring frequent observations of terrestrial surfaces in both the solar and thermal bands.
- Climatological applications and climate change detection, requiring long and homogeneous time-series.

Table 1. The LSA SAF Set of Products and respective sensors and platforms. The table covers both existing and future EUMETSAT satellites, and therefore refers operational products and development activities.

| Product Family | Product Group | Sensors/Platforms |
|---|---|---|
| **Radiation** | Land Surface Temperature (LST) | SEVIRI/MSG, AVHRR/Metop, FCI/MTG, VII/EPS-SG |
| | Land Surface Emissivity (EM) | SEVIRI/MSG, FCI/MTG (internal product for other sensors) |
| | Land Surface Albedo (AL) | SEVIRI/MSG, AVHRR/Metop, FCI/MTG, VII/EPS-SG, 3MI/EPS-SG |
| | Down-welling Short-wave Fluxes (DSSF) | SEVIRI/MSG, FCI/MTG |
| | Down-welling Long-wave Fluxes (DSLF) | SEVIRI/MSG, FCI/MTG |
| **Vegetation** | Normalized Difference Vegetation Index (NDVI) | AVHRR/Metop, VII/EPS-SG |
| | Fraction of Vegetation Cover (FVC) | SEVIRI/MSG, AVHRR/Metop, FCI/MTG, VII/EPS-SG, 3MI/EPS-SG |
| | Leaf Area Index (LAI) | SEVIRI/MSG, AVHRR/Metop, FCI/MTG, VII/EPS-SG, 3MI/EPS-SG |
| | Fraction of Absorbed Photosynthetically Active Radiation (FAPAR) | SEVIRI/MSG, AVHRR/Metop, FCI/MTG, VII/EPS-SG, 3MI/EPS-SG |
| | Gross Primary Production (GPP) | SEVIRI/MSG, FCI/MTG |
| | Canopy Water Content (CWC) | AVHRR/Metop, VII/EPS-SG |
| **Energy Fluxes** | Evapotranspiration (ET) | SEVIRI/MSG, FCI/MTG |
| | Reference Evapotranspiration (ET0) | SEVIRI/MSG, FCI/MTG |
| | Surface Energy Fluxes: Latent and Sensible (LE&H) | SEVIRI/MSG, FCI/MTG |
| **Wild Fires** | Fire Detection and Monitoring (FD&M) | SEVIRI/MSG |
| | Fire Radiative Power | SEVIRI/MSG, FCI/MTG, VII/EPS-SG |
| | Fire Radiative Energy and Emissions (FRE) | SEVIRI/MSG, FCI/MTG, VII/EPS-SG |
| | Fire Risk Map (FRM) | SEVIRI/MSG, FCI/MTG |

| | | |
|---|---|---|
| | Burnt Area (BA) | AVHRR/Metop, VII/EPS-SG |

The LSA SAF products (Table 1) are based on level 1.5 SEVIRI/Meteosat and/or level 1b MetOp data. Forecasts provided by the European Centre for Medium-range Weather Forecasts (ECMWF) are also used as ancillary data for atmospheric correction.
The SEVIRI/Meteosat derived products are generated for the full Meteosat disk. However the NRT dissemination via EUMETCast is made by splitting the full disk into 4 geographical areas within Meteosat disk (Figure 1)

- Euro – Europe, covering all EUMETSAT member states;
- NAfr – Northern Africa encompassing the Sahara and Sahel regions, and part of equatorial Africa.
- SAfr – Southern Africa covering the African continent south of the Equator.
- SAme – South American continent within the Meteosat disk.

MetOp derived parameters are currently available at level 1b full spatial resolution and for the processed Product Distribution Units (PDUs), each corresponding to about 3 minutes of instrument-specific observation data.

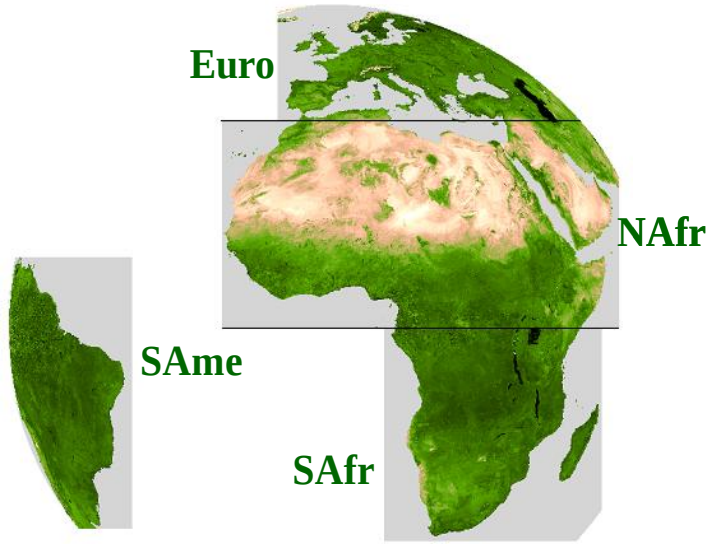


Figure 1 - The LSA SAF geographical areas.

The LSA SAF system is fully centralized at IPMA and will be able to operationally generate, archive, and disseminate the operational products. The monitoring and quality control of the operational products, also centralized at IPMA, is performed automatically by the LSA SAF software, which provides quality information to be distributed with the products.

The LSA SAF products are currently available from LSA SAF website (http://landsaf.meteo.pt) that contains real time examples of the products as well as updated information.

This document is one of the product manuals dedicated to LSA SAF users. The algorithm and the main characteristics of the Evapotranspiration (ET) generated by the LSA SAF from SEVIRI data system is described in the following sections. The characteristics of SEVIRI based ET products provided by the LSA SAF are described in (Table 1) Further details on the LSA SAF product requirements may be found in the Product Requirements Document (PRD) available at the LSA SAF website (http://landsaf.ipma.pt)

| ET Product | Product Identifier | Coverage | Resolution | | Accuracy | | |
|---|---|---|---|---|---|---|---|
| | | | Temporal | Spatial | Threshold | Target | Optimal |
| MET: ET_SEVIRI | LSA-16 | MSG disk | 30 min | MSG pixel resolution | 30% | MET>0.4 mm/h: 25%; MET<0.4 mm/h: 0.1 mm/h | 10% |
| DMET: ET_SEVIRI | LSA-17 | MSG disk | 1 day | MSG pixel resolution | 30% | 20% | 10% |

**Table 2 Product Requirements for ET, in terms of area coverage, resolution and accuracy.**

A synthesis is presented hereafter about the adopted methodology (chapter 2) and validation results (chapter 4). However, in order to get more detailed information, interested users can refer to the related documentation:

- Algorithm Theoretical Basis Document (ATBD) for MET (LSA-16) and DMET (LSA-17);
- Validation report for MET (LSA-16) and DMET (LSA-17), both available from the LSA SAF website.

# 2 Algorithm description

## 2.1 Instantaneous product (MET)

Information consigned in this document, concerns two evapotranspiration products: The instantaneous ET estimates, with a time interval of 30 minutes (MET), currently generated with the version 4.0.7 of the MET algorithm and the daily evapotranspiration product (DMET) derived by integrating instantaneous values over the whole day. This later product is generated with a common algorithm used for the integration over days of LSA SAF derived radiative fluxes (DSSF, DSLF). The main difference between current document and its previous version is the inclusion of information concerning the daily product (chapter 2.2) and some modifications in the metadata of the instantaneous product. Daily product is generated over the four windows defined inside the MSG disk.

### 2.1.1 Overview

The EvapoTranspiration (ET) algorithm developed in the framework of LSA-SAF, targets the quantification of the flux of water vapour from the ground surface (soil and canopy) into the atmosphere using input data derived from MSG satellites. The method follows a physical approach and can be described as a simplified Soil-Vegetation-Atmosphere Transfer (SVAT) module modified to accept as forcing Satellite Remote Sensing (SRS) derived data combined with data from other sources mainly NWP.

### 2.1.2 Physics of the problem

Evapotranspiration is one of the main components of the water cycle and it is directly associated with the latent heat flux (LE), which establishes a key link between the energy and water cycles. Evaluating energy fluxes at the Earth surface is of great importance in many disciplines like weather forecasting, global climate monitoring, water management, agriculture, ecology, etc. When dealing with ET at specific locations or at small watershed scales, most of the proposed methods are based on classical measurements of eddy correlation, Bowen ratio, and soil-water balance, supported by a network of ground stations.

At regional and global scales, the satellite remote sensing (SRS) stays as the only method capable to provide wide area coverage at economically affordable costs. Most of proposed methods use SRS derived data combined into models with different degrees of complexity. These models rang from empirical direct methods to complex deterministic models based on SVAT modules that compute the different components of the energy budget. A major difficulty to the use of SRS for monitoring ET is that the phase change of water molecules produces neither emission nor absorption of an electromagnetic signal. Therefore the ET process is not directly quantifiable from satellite observations. It has to be assessed, taking advantage of information gained through the satellite about surface variables influencing evapotranspiration (Choudhury, 1991).

### 2.1.3 Proposed method

In the proposed method, the area for which ET has to be assessed is divided into independent pixels, in a one-to-one correspondence with the pixels of a satellite image. Each pixel is in turn considered as being a mix of homogeneous *tiles*, each tile representing a particular soil surface: bare soil, grassland, forests, *etc*. In Figure 2, a schematic representation of the image pixel composition is presented. In the model, some variables are defined at the pixel level and are thus shared by all the tiles composing the pixel, while others are defined at the tile level. Intermediate variables (aerodynamic resistance, Obukhov length, friction velocity) are computed at the tile level (see next section). The global pixel value is obtained through the weighted contribution of each tile. Theoretically, ET can be derived in near real time at the time resolution of MSG satellite images, in practice, the generation of ET will be limited by the availability of input data (DSLF is generated every 30 minutes). In the current version, snow sublimation is not modelled. Permanently snow covered pixels are labelled as not processed. For snow events only evapotranspiration from the vegetation is considered.

***Figure 2 Schematic representation of pixel composition***

### 2.1.4 Mathematical description of the algorithm

The main set of equations used for deriving ET are common to most SVAT schemes with specific parameterizations adopted from the ECMWF TESSEL SVAT scheme (van den Hurk et al., 2000) in which some adaptations have been done in order to use SRS derived data. For a detailed mathematical description of the algorithm, please refer to the Algorithm Theoretical Basis Document (ATBD).

#### 2.1.4.1 At tile level

Neglecting the energy storage into the vegetation layer, each tile satisfies an energy balance given by

$$Rn_i = H_i + LE_i + G_i \qquad (1a)$$

with

$$Rn_i = (1-\alpha)S_{\downarrow} + \varepsilon(L_{\downarrow} - \sigma T_{sk,i}^4) \qquad (1b)$$

In these equations, the index *i* refers to a given tile, $\alpha$ and $\varepsilon$ are respectively albedo (from LSA-SAF ALbedo product) and emissivity (0.99 by now, LSA-SAF Emissivity is foreseen to be used in future versions), $S_{\downarrow}$ and $L_{\downarrow}$ the Downward Surface Short-wave Flux (DSSF) and the Downward Surface Long-wave Flux (DSLF), $H_i$ and $LE_i$ are the sensible and latent heat fluxes respectively, $G_i$ is the heat flux into the soil, $T_{sk,i}$ the skin temperature and $\sigma$ is the

Stephan-Boltzmann constant. $R_{ni}$, $S_{\downarrow}$,and $L_{\downarrow}$ are positive downward whereas $H_i$, $LE_i$,and $G_i$ are positive upward.

The latent and sensible heat fluxes are obtained via a resistance analogy:

$$LE_i = \frac{L_v \rho_a}{(r_a + r_c)}\left[q_{sat}(T_{sk,i}) - q_a(T_a)\right] \quad (2)$$

$$H_i = \frac{\rho_a}{r_a}\left[c_p(T_{sk,i} - T_a) - gz_a\right] \quad (3)$$

where $\rho_a$ is the air density, $r_a$ the aerodynamic resistance, $T_a$ is the air temperature, $z_a$ the measurement height of the air parameters, $r_c$ the canopy resistance, $L_v$ the latent heat of vaporisation (function of the air temperature), $q_a$ the specific humidity and $q_{sat}$ is the specific humidity at saturation. The canopy resistance $r_c$ is a function of DSSF, leaf area index (LAI), average unfrozen soil water content (θ), atmospheric water pressure deficit and a minimum stomatal resistance ($r_{s,min}$).

The heat flux into the ground is estimated according to

$$G_i = \beta_i * Rn_i \quad (4)$$

In this equation coefficient $\beta_i$ is estimated as a function of Leaf Area Index (LAI), through the Modified Soil Adjusted Vegetation Index -MSAVI- (Chehbouni et al., 1996) as following

$$\beta_i = 0.5 * EXP(-2.13 * MSAVI_i) \quad (5)$$

$$MSAVI_i = 0.88-0.78*EXP(-0.6 * LAI_i) \quad (6)$$

### 2.1.4.2 At pixel level

$$LE = \sum \zeta_i LE_i \quad \text{and} \quad H = \sum \zeta_i H_i \quad (7)$$

where $\zeta_i$ is the relative coverage of the tile in the pixel.

The LE obtained, expressed in W/m², is converted in evapotranspiration (in mm/h) by means of

$$ET = 3600\ LE/Lv. \quad (8)$$

Snow sublimation is not yet considered

### 2.1.5 Input data

#### 2.1.5.1 Radiative data

The main radiative variables driving the model are taken from corresponding LSA-SAF products. These variables are at first the Downward Surface Short-wave Flux (DSSF) based on the three short-wave channels (VIS 0.6µm, NIR 0.8µm, SWIR 1.6µm); for more details see the DSSF (PUM) document. Secondly, the Downward Surface Long-wave Flux (DSLF) is obtained by an hybrid method based on two different bulk parameterisation schemes for clear and cloudy sky conditions using as input ECMWF forecasts of 2m temperature, 2m dew point temperature and total column water; for details see the DSLF (PUM) document. Finally, the albedo (AL) product is used as input. It is based on the three short-wave channels (VIS 0.6µm, NIR 0.8µm, SWIR 1.6µm). For more details see the albedo (PUM) document.

#### 2.1.5.2 Meteorological data

Meteorological auxiliary data needed by the MET algorithm is automatically retrieved from ECMWF forecasts by the processing modules of the LSA-SAF system. This data originally gathered at ECMWF spatial resolution is transposed into the MSG grid and spatially interpolated. Currently, the meteorological variables used by the MET algorithm are:

- 2-m temperature [K]
- 2-m dew point temperature [K]
- 10-m wind speed [m/s]
- Atmospheric pressure at sea level [Pa]
- Soil moisture for 4 soil layers [$m^3$/ $m^3$]
- Soil temperature for 4 soil layers [K]

#### 2.1.5.3 Land cover

The version 4.0.7 of the MET algorithm uses the ECOCLIMAP (Masson et al., 2003) land cover classification, resampled onto MSG spatial resolution (original ECOCLIMAP resolution is one kilometre). In this database, the parameters associated to a given tile vary temporally (on monthly basis) and spatially (parameters associated to tiles depend on the considered climatic region). In Figure 3 the first and second predominant vegetation types (tiles) used by the LSA-MET algorithm are presented.

In the present method, up to three different tiles are allowed on each single grid point (see Figure 3), this to provide a more realistic surface description compared to the restriction to dominant land cover type. This approach is particularly relevant in very patchy landscapes. In the current version, the following ECOCLIMAP fields have been exploited: land cover types, fraction of vegetation cover, LAI and roughness length.

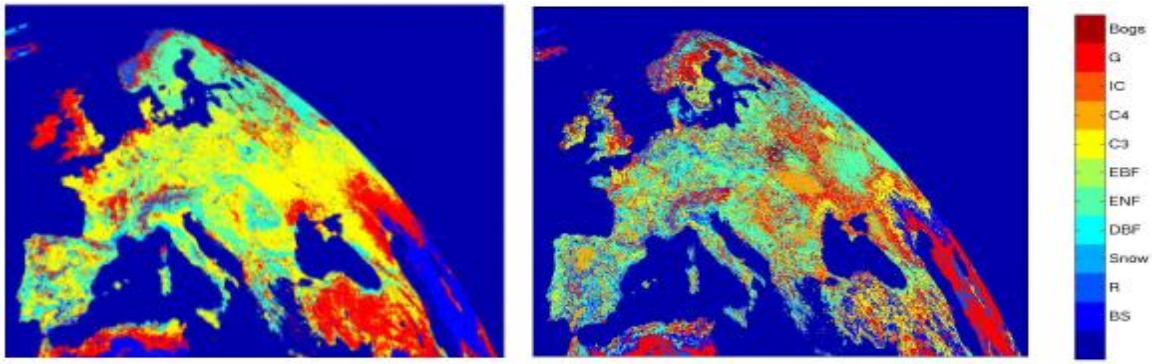


***Figure 3 First (left) and second (right) vegetation types used by the LSA SAF ET algorithm. 'Bogs' stands for bogs/swamp vegetation/gardens, 'G' for grass land, 'IC' for irrigated crops, 'C4' for C4 crops, 'C3' for C3 crops, 'EBF' for evergreen broadleaf forest, 'ENF' for evergreen needle leaf forest, 'DBF' for deciduous broadleaf forest, 'Snow' for permanent snow, 'R' for rocks and 'BS' bare soil.***

### 2.1.6 Processing scheme

The algorithm execution may be decomposed in three steps represented at Figure 4 by a schematic flowchart. The first step corresponds to the pre-processing. At this stage, the algorithm verifies that all necessary input data is available, executes the gap filling procedure over missing DSLF pixels values over land, initialises internal structures and loads input data into internal arrays. The second step is the equations solving process. Here the algorithm starts with the first pixel on the image. If all necessary input data is available, the algorithm solves the set equations for each tile and, if convergence is reached, computes ET for the whole pixel. Based on the quality of input data and the performances of the algorithm itself, a quality flag value is calculated for the pixel. The third step is output formatting. Here the algorithm sets the scaling factor for the whole image, performs data type casting, set the data and attributes and writes the output in HDF5 formats, following. Then, the algorithm frees used memory, returns control to the wrapper and stands idle till next call.

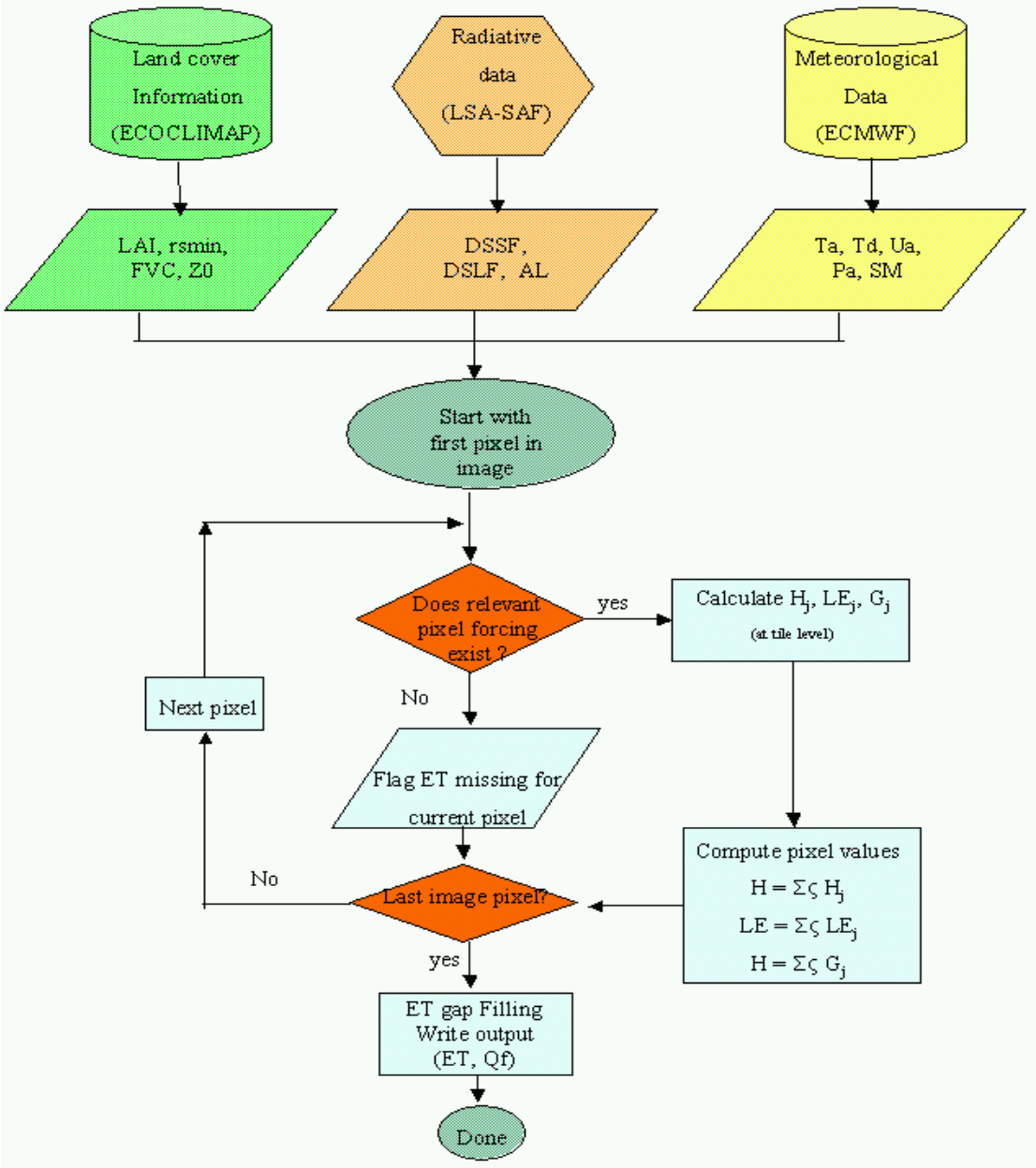


***Figure 4 Diagram of ET processing chain.***

### 2.1.7 Error budget estimates

A first source of uncertainties is introduced by the physical formalism of the algorithm itself. Another important source of uncertainties results from the errors associated to the error in the estimation of input variables and particularly DSSF, DSLF, albedo, air temperature, specific humidity, wind speed, etc. From a global point of view, the main sources of uncertainties cumulated on the ET product deal with sensors performance, accuracy of cloudy pixels

identification, accuracy of atmospheric corrections, surface heterogeneity and land cover classification.

In order to evaluate the impact of input variables uncertainties on the estimation of the ET algorithm performances, an extensive sensitivity analysis is performed over the main input variables. In this test, the ET algorithm is run 5000 times with a time step of 30 minutes over a selected dataset at the Cabauw site. The test consists in running the ET model allowing the input variables to vary randomly over its range of possible values, with a dispersion determined by the maximum possible error specified for a given variable: DSSF - 15 W/m² by clear sky conditions, DSLF and Albedo - 10% of the actual value as specified by products developers.

A global sensitivity study of all input variables varying simultaneously concludes that the total error induced on ET is lower than the sum of individual contributions. A soil moisture analysis revealed that ET algorithm is very sensitive to this variable, especially for dry regions for which soil water availability is the main limiting factor. Among variables coming from LSA-SAF, DSSF is the most important driver for the ET. Figure 5 shows the relation between the range of DSSF values and the relative error induced on ET by uncertainty on input variables. We see that for high DSSF values (greater than 350 W/m2) introduced error is less than 10%. A detailed discussion about error and uncertainties due to input variables (DSLF, AL, air temperature, air humidity, wind speed) is included in the Validation Report (VR).

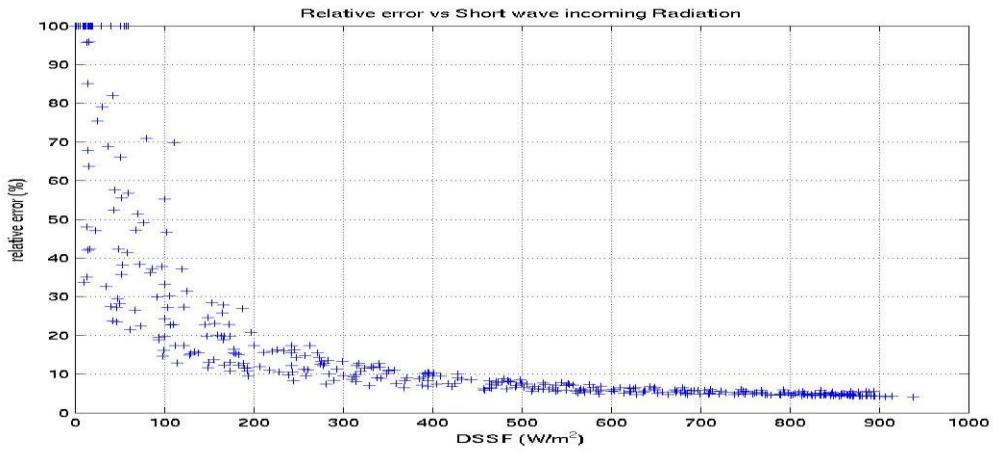


***Figure 5 Relation between DSSF range of values and relative error induced on ET by uncertainty on input variables.***

## 2.2 Daily product (DMET)

The daily evapotranspiration product is obtained by temporal integration of instantaneous values (equation 9). The implemented procedure accounts for missing slots/values by allowing pixels evapotranspirate at a rate equivalent to the average between two existing slots (one previous the other after the missing slot/value)

$$DMET = \int_{h_1}^{h_2} MET_i(t)\,dt \qquad (9)$$

Where $MET_i$ is the instantaneous evapotranspiration estimated, the integration limits ($h_1$, $h_2$) correspond to the first (theoretically at 00:30 UTC) and last (theoretically at 24:00 UTC) existing slots for a given day, *dt* is the integration step (30 minutes). In optimal situation (no missing slots) 48 images are integrated for a given day.

# 3 Product description

## 3.1 Product content

**Instantaneous product**. The ET algorithm produces evapotranspiration estimates in mm/h over the four LSA-SAF defined windows at MSG/SEVIRI spatial resolution and a time step of 30 minutes. Together with the ET map, a quality flag image is also generated. This image has the same size as the ET image and provides information on pixel-by-pixel basis about the confidence of estimated values. It informs about the quality of input variables and if pre/post-processing (gap filling) was performed on input or output data (see chapter 3.5). After each algorithm execution, four output files are generated. Each of them is labelled: "HDF5_LSASAF_MSG_ET_Area_yyyymmddhhhh", with 'Area' being one of 'Euro', 'NAfr', 'SAfr' or 'Same')

Figure *Figure* 6 shows ET estimates over Europe and the corresponding quality flag images for the day 2007/08/01 at 12:00 UTC. Images corresponding to North Africa, South Africa and South America are represented at Figures 7, 8 and 9 respectively.

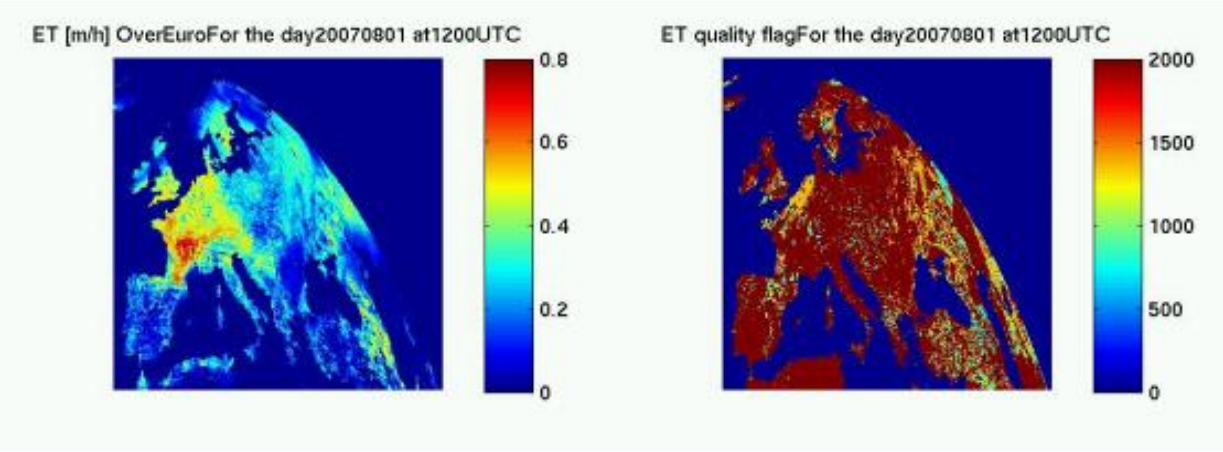


***Figure 6 ET image over Europe (left) and corresponding quality flag image (right) for the 1st August 2007 at 12 h UTC.***

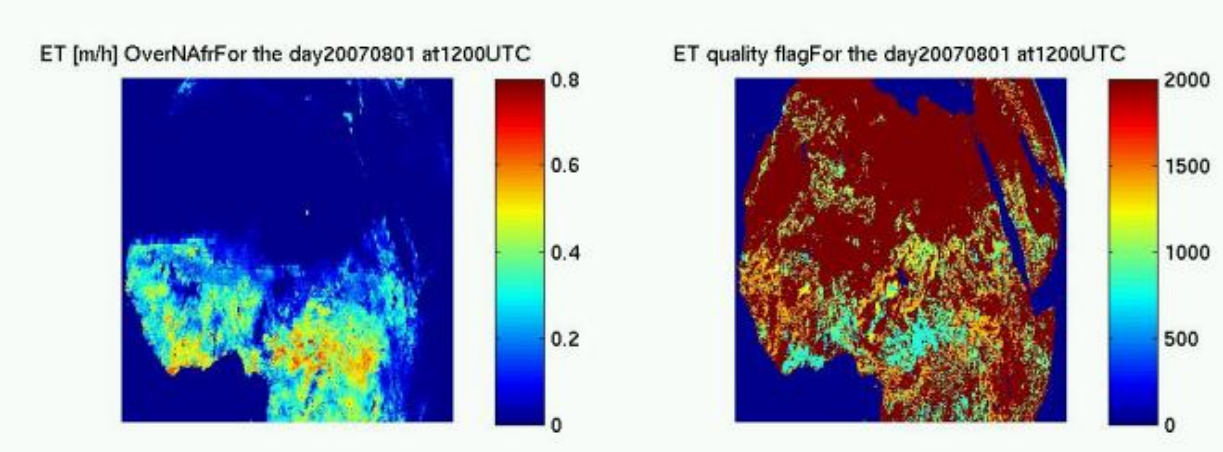


***Figure 7 ET image over Northern Africa (left) and corresponding quality flag image (right) for the 1st August 2007 at 12 h UTC.***

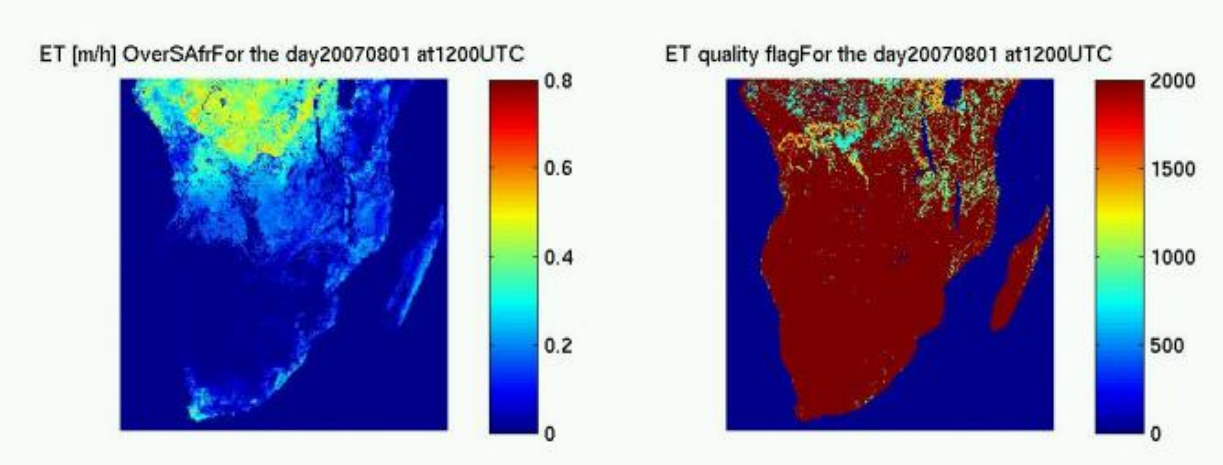


***Figure 8 ET image over Southern Africa (left) and corresponding quality flag image (right) for the (right) for the 1st August 2007 at 12 h UTC.***

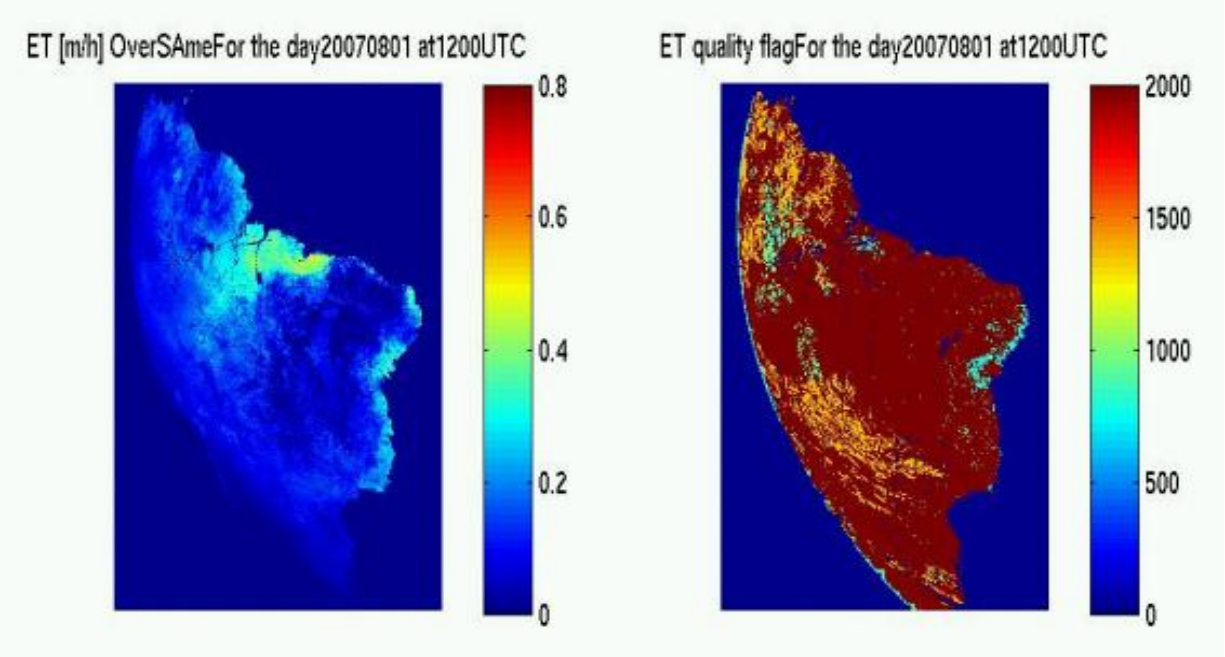


***Figure 9 ET image over Southern America (left) and corresponding quality flag image (right) for the 1st August 2007 at 12 h UTC***

**Daily product**. The daily product is generated with a lag time of one day. Every output file is composed of 3 images containing DMET estimates, information about the percentage of missing values for every pixel on the image and information about the number of missing slots for a given day. In figure 10 below, an example of the DMET product and the accompanying information on missing values is presented for 10th September 2010 over the full MSG disk.

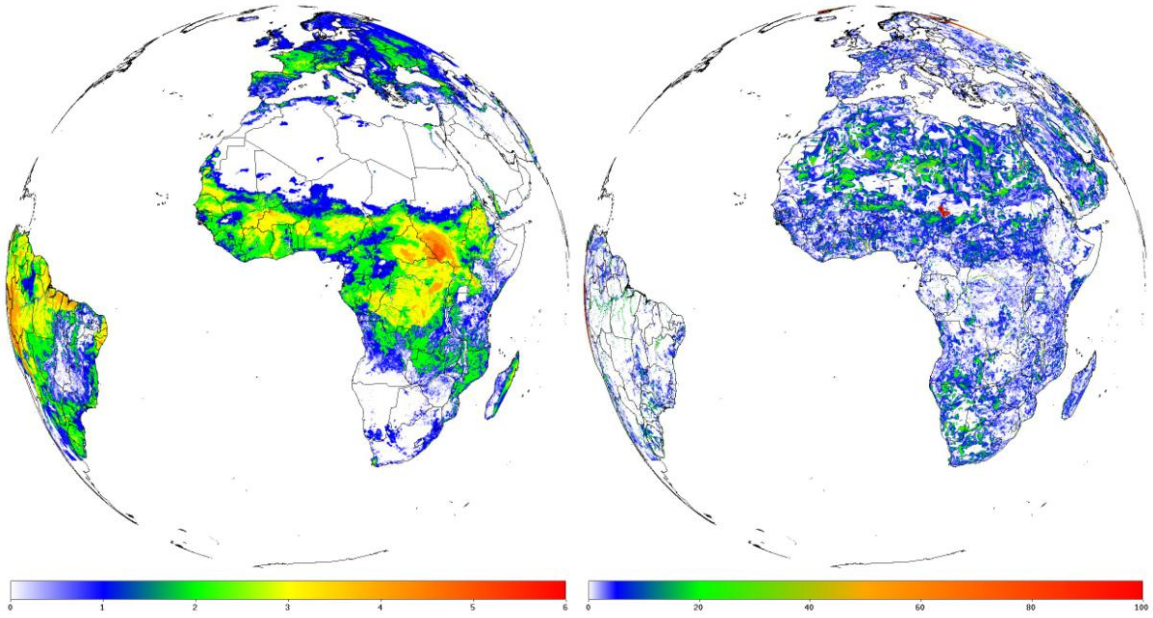

***Figure 10 DMET (mm) product (on left ) and the missing (%) pixels information image (on right) for 10th September 2010 over full MSG disk.***

## 3.2 Files format

The data format used by the LSA-SAF consortium is the Hierarchical Data Format, version 5 (HDF5), developed by the National Centre for Supercomputing Applications (NCSA). This is a public, general-purpose and machine independent standard for storing and sharing scientific data. In this format, each file contains also the necessary information for manipulating the data. General attributes common to all LSA SAF products are described in Annex A. The latest version of HDF5 libraries for several platforms can be found in ftp://ftp.ncsa.uiuc.edu/HDF/HDF5/hdf5-1.6.2/. A free software to open and view HDF5 files is available in http://hdf.ncsa.uiuc.edu/hdf-java-html/hdfview/.

## 3.3 Geolocation / Rectification

The **ET** SEVIRI-based fields are generated pixel-by-pixel, maintaining the original resolution of SEVIRI level 1.5 data. These correspond to rectified images to 0º longitude, which present a typical geo-reference uncertainty of about 1/3 of a pixel. Data are kept in the native geostationary projection.

Files containing the latitude and longitude of the centre of each pixel may be downloaded from the Land-SAF website (http://landsaf.ipma.pt; under "Static Data and Tools"):

**Longitude**

HDF5_LSASAF_MSG_LON_MSG-Disk_201408100000.bz2
HDF5_LSASAF_MSG_LON_Euro_200512201600.bz2
HDF5_LSASAF_MSG_LON_NAfr_200505191503.bz2
HDF5_LSASAF_MSG_LON_SAfr_200505191525.bz2
HDF5_LSASAF_MSG_LON_SAme_200505191527.bz2

**Latitude**

HDF5_LSASAF_MSG_LAT_MSG-Disk_201408100000_.bz2
HDF5_LSASAF_MSG_LAT_Euro_200512201600.bz2
HDF5_LSASAF_MSG_LAT_NAfr_200505191503.bz2
HDF5_LSASAF_MSG_LAT_SAfr_200505191525.bz2
HDF5_LSASAF_MSG_LAT_SAme_200505191527.bz2

Alternatively, since the data are in the native geostationary projection, centred at 0º longitude and with a sampling distance of 3 km at the sub-satellite point, the latitude and longitude of any pixel may be easily estimated. Given the pixel column number, *ncol* (where *ncol*=1 corresponds to the westernmost column of the file), and line number, *nlin* (where *nlin*=1 corresponds to the northernmost line), the coordinates of the pixel may be estimated as follows:

$$lon = arctg\left(\frac{s_2}{s_1}\right) + sub\_lon$$ longitude (deg) of pixel centre

$$lat = arctg\left(p_2 \cdot \frac{s_3}{s_{xy}}\right);$$ latitude (deg) of pixel centre

where sub_lon is the sub-satellite point ( $sub\_lon = 0$ )
and

$$s_1 = p_1 - s_n \cdot \cos x \cdot \cos y$$

$$s_2 = s_n \cdot \sin x \cdot \cos y$$

$$s_3 = - s_n \cdot \sin y$$

$$s_{xy} = \sqrt{s_1^2 + s_2^2}$$

$$s_d = \sqrt{(p_1 \cdot \cos x \cdot \cos y)^2 - (\cos^2 y + p_2 \cdot \sin^2 y) \cdot p_3}$$

$$s_n = \frac{p_1 \cdot \cos x \cdot \cos y - s_d}{\cos^2 y + p_2 \cdot \sin^2 y}$$

where

$$x = \frac{ncol - COFF}{2^{-16} \cdot CFAC} \quad \text{(in Degrees)}$$

$$y = \frac{nlin - LOFF}{2^{-16} \cdot LFAC} \quad \text{(in Degrees)}$$

$p_1 = 42164$

$p_2 = 1.006803$

$p_3 = 1737121856$

$CFAC = 13642337$

$LFAC = 13642337$

The CFAC and LFAC coefficients are column and line scaling factors, which depend on the specific segmentation approach of the input SEVIRI data. Finally, COFF and LOFF are coefficients depending on the location of the each Land-SAF geographical area within the Meteosat disk. These are included in the file metadata (HDF5 attributes; Annex A), and correspond to one set of the values detailed below per SEVIRI/MSG area:

| Region Name | Description | Maximum *ncol* | Maximum *nlin* | COFF | LOFF |
|---|---|---|---|---|---|
| MSG-Disk | Full MSG Disk | 3712 | 3712 | 1857 | 1857 |
| Euro | Europe | 1701 | 651 | 308 | 1808 |
| NAfr | Northern Africa | 2211 | 1151 | 618 | 1158 |
| SAfr | Southern Africa | 1211 | 1191 | -282 | 8 |
| SAme | Southern America | 701 | 1511 | 1818 | 398 |

**Table 3 Maximum values for number of columns (ncol) and lines (nlin), for each Land-SAF geographical area, and the respective COFF and LOFF coefficients needed to geo-locate the data.**

## 3.4 Summary of product characteristics

### 3.4.1 Instantaneous product

Product Name: Evapotranspiration

Product Code: ET

Product Level: Level III

Description of Product**:** Evapotranspiration from surface into the atmosphere

**Product Parameters:**

Coverage: Full disk (land pixels)

Units: mm/h

Range: 0 – 1

Sampling: pixel by pixel basis

Spatial Resolution: MSG full resolution (3km×3km at nadir)

Accuracy: 25% if ET >0.4 mm/h;
0.1 mm/h else.

Geo-location Requirements:

Format: 16 bits signed integer

Appended Data: Quality control information (16 bits integer)

Frequency of generation: 30 min

Size of Product:

| | | |
|---|---|---|
| MSG-Disk: | (Non-compressed) | 26.28 MB |
| Europe: | (Non-compressed) | 4.23 MB |
| North Africa | (Non-compressed) | 9.72 MB |
| South Africa: | (Non-compressed) | 5.52 MB |
| South America: | (Non-compressed) | 4.05 MB |

**Additional Information:**

Identification of bands used in algorithm: Not applicable

Assumptions on SEVIRI input data: Not applicable

Identification of MSG derived data:

- Downward Surface Short-wave Flux (DSSF)
- Surface Albedo (AL)
- Downward Surface Long-wave Flux (DSLF)

Identification of ancillary and auxiliary data:

- Land-sea mask
- 2-m temperature (from ECMWF)
- 2-m dew point temperature (from ECMWF)
- Wind speed (from ECMWF)
- Atmospheric pressure al sea level (from ECMWF)
- Soil moisture for 4 soil layers (from ECMWF)
- Soil temperature for 4 soil layers (from ECMWF)
- ECOCLIMAP land cover database

### 3.4.2 Daily product

Characteristics of daily product such as file format, product level, coverage, sampling and size of the product remain the same as for instantaneous product. Here below we summarize the characteristics that are different from those of the instantaneous product:

Product Name: Daily Evapotranspiration

Product Code: DMET

Units: mm/day

Range: 0 – 10

Accuracy: 20 %

Frequency of generation: daily

Appended Data: Information about missing slots and missing values(16 bits integer)

## 3.5 Quality indices

Each ET field is associated with a quality flag index, coded in 16-bit word. The expected values for quality control flag as well as their meaning are described in Annex B. Only fields related to land/sea mask (bit 0), land cover (bit 1), AL (bit 7), DSLF (bit 10-11), DSSF (bit 12-13), and ET (bit 14-15) are used. Non-used bits are set to 0. The quality of the ET output is defined as: nominal, below nominal, poor or non-processed:

1) Nominal:
   - The quality flag of all LSA-SAF (DSSF, DLSF, ALBEDO) variables is at least nominal and
   - ET algorithm processed correctly

Possible values: 1349 and higher

2) Below nominal:
- DLSF gaps filled in pre-processing (quality flag set to 965)
- The quality of at maximum one of LSA-SAF variable is below nominal

Possible values: between 965, and 1285

3) Poor quality:
- The quality of more than one LSA-SAF variable is below nominal and/or
- LSA-SAF AL non-processed (Albedo taken from ECOCLIMAP database)
- Gaps filled in post-processing (quality flag set to 800)

Possible values: 581, 645, 709, 800

4) Non-processed:
-Pixel on the sea/water
-Missing input variables and
-Not gap filled in pre/post-processing
-Algorithm failure (no convergence)

Possible values: values below 100. Non processed pixels over land are set with the quality flag minus one (-1) and over sea/water minus two (-2).

For the daily product, no quality indices are provided. Instead, information about the percentage of missing values on pixel-by-pixel basis is included in an accompanying image.

### 3.6 Gap filling procedure

In order to provide ET with a limited amount of missing values, a gap filling procedure is implemented in pre-processing (for land pixels where DLSF is not available) and post processing (for land pixels for which it is not possible to calculate ET, because of missing input variables or no convergence of the algorithm). The gap filling procedure estimates the value for a given pixel based on the neighbouring pixels values weighted by distance (closest pixels have more weight). The quality flag for those pixels is set to a default value of 965 (below nominal) if DSLF was initially missing or to 800 (poor) if pixel ET value is obtained by interpolation from post-processing.

## 4 Validation

In this chapter we present shortly the different validation tests done in order to assess the performances and limitation of the proposed method. For a detailed description of the validation procedure and recent results please refer to the Validation Report on the LSA-SAF web site (http://landsaf.ipma.pt/). Main conclusions from validation report are included in annexe C. Three validation strategies have been adopted in order to assess the accuracy of the produced evapotranspiration values:

- Off-line validation
- Continuous validation
- Comparison with output from reference models

## 4.1 Off-line validation.

The output of the algorithm run in stand-alone mode is compared to observations of reference sites from known measurements networks like CarboEurope, CEOP, the Belgian Automatic Weather Stations (AWS) network, etc. Local observations are used as input as well as local available parameters. Details in validation report, Annex C, (Off-line Validation of the 0-D LSA-SAF MET v4.0 algorithm)

## 4.2 Comparison with ground reference

### 4.2.1 Instantaneous product (MET)

The output of the on-line version of the algorithm is compared for tiles to measurements on selected locations. In order to closely follow the performances of the algorithm, a set of 120 sites were predefined over Europe (75 for other MSG disk regions) with results saved on separated validation files. In Figure11, the scatter plots of 30 minutes observations vs simulation are presented for four different sites (Cabauw, Wetzstein, Kaamanen an Vielsalm) from the CarboEuroIP network over Europe. Uncertainty bounds are also included as well as statistical indices. They are given by the "target accuracy" (Table 2), also included in the Product Requirements Document (PRD).

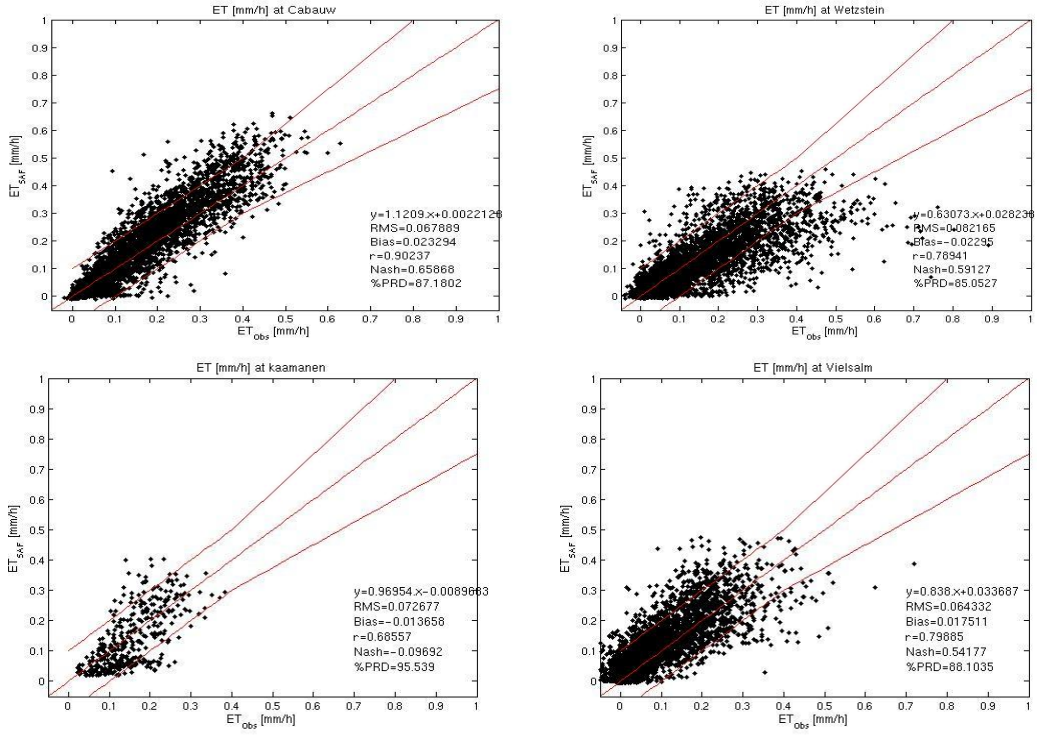

***Figure11 Comparison of LSA-SAF MET tiled estimates with in-situ measurements.***

### 4.2.2 Daily product (DMET)

The daily product has been validated by comparing the output of the DMET algorithm to daily-cumulated values at selected reference sites. To show the coherence between both products, and owing to data availability issues, the reference sites used for DMET product are the same used for MET validation. Three types of plots have been generated: Ten days sliding averages, scatter plots with superimposed statistical indicators and Taylor diagrams (Taylor, 2001). Figure 12 represents the generated plots for the station of Vielsalm in 2007 (more details in validation report).

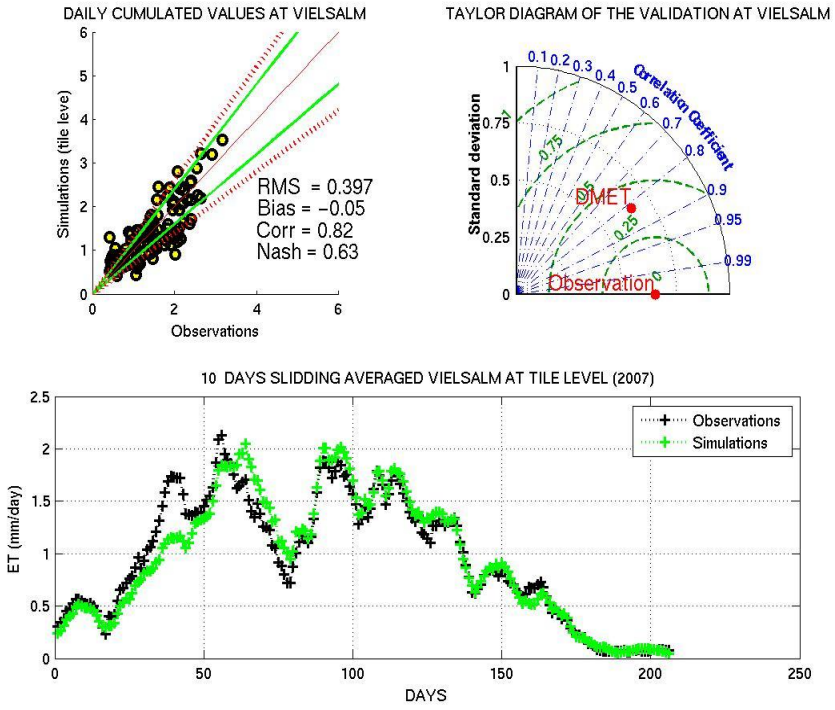


***Figure 12 Comparison of DMET product to daily-cumulated ET values at Vielsalm station for 2007.***

## 4.3 Inter-comparison with other products.

### 4.3.1 Instantaneous product (MET)

LSA-SAF ET estimates cumulated over 3 hours (6 images by estimate) are compared to 3-hourly ECMWF and GLDAS output. 3 types of statistical tests have been performed: One-to-

one comparison of images, global analysis of images over a long period and finally a regionalized statistical test to determine the differences between models predictions over different biomes.

From Figure 13 we observed that LSA-SAF MET estimates are globally in agreement with ET estimates provided by ECMWF and GLDAS, with a high spatial correlation, ranging between 85% and 95% for mid-day images through the whole period, i.e. 01/03/2007 to 30/11/2007. While similarity with GLDAS is observed in case of low solar co-zenithal angle, i.e. early spring/late autumn and morning/evening, summer estimates correlates better with ECMWF. A slight bias found in comparisons with ECMWF can be correlated with a bias in global radiation at surface. We clustered the different geographical regions where differences in time series are noticeable. Most of the differences observed are not systematic: large disparities exist between ECMWF and GLDAS. Most of the ET differences can be explained in terms of differences of input variables/parameters, i.e. incoming global radiation at surface, land cover and resistance to transpiration of the canopy, function of LAI. While global radiation at the surface is the main source of difference on short-term basis, vegetation characteristics and soil moisture act on long-term basis and cause major ET differences observed. LSA-SAF MET estimates over Europe behave in a reasonable range compared to ECMWF and GLDAS. Most of the differences between models output have been attributed to differences in input variables/parameters, indicating that models performances are similar. Figure 13 encompasses the mean distribution of the 3 hourly averaged ET (09UTC to 12UTC) for MET, ECMWF and GLDAS for the months of April and July 2007. The mean value of the distribution is represented by the red lines.

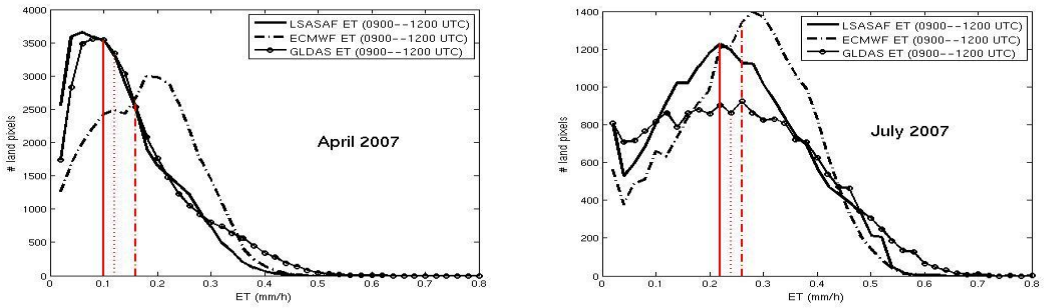


***Figure 13 Distributions of ET estimates from LSA-SAF ET (solid line), ECMWF (dash-dotted line) and GLDAS (solid line and circles).***

### 4.3.2 Daily product (DMET)

For the comparison at regional scale, the output of the DMET algorithm was compared to daily ET cumulates from ECMWF. Based on results of the instantaneous product validation DMET algorithm is expected to produce daily ET estimates with accuracy equivalent to the accuracy of instantaneous product. In figure 14 the spatial correlation, between DMET and ECMWF estimates, is presented for December 2009. Conclusions of the validation report are included in annexe C.

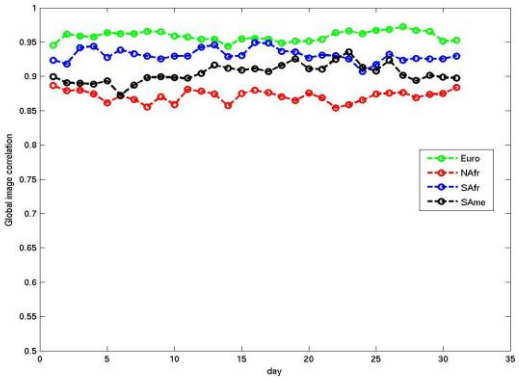


***Figure 14 Spatial correlation between DMET and ECMWF images for the month of December 2009, over Europe (green), North Africa (red), South America(black) and South Africa(blue).***

## 5 Concluding remarks

Based on the results of the validation exercise (see annexe C), it is concluded that the ET algorithm is able to reproduce the temporal evolution of evapotranspiration with values comparable with observations. Good agreement was found for stations over grassland and mixed forest and globally for stations where the cover type at station corresponds closely to the cover type defined in the land cover database used in the model.

From the inter-comparison with ECMWF and GLDAS models, no evidence of systematic bias was observed. A compliance with PRD quality criterion is satisfied to a rate generally higher than 70%, for estimates flagged nominal and below nominal. The mismatches were attributed to differences in solar radiation, vegetation characteristics, considered soil water availability and spatial scales of the compared models output.

The accuracy of the DMET product is directly related to the accuracy and continuity in the generation of instantaneous product. DMET fairly matches the observed variations, with a very good agreement with observations for well-watered sites and a good seasonal variation for temperate forests. The comparisons of DMET to ECMWF daily-accumulated ET confirm the results obtained during the validation of instantaneous product. From the comparisons achieved until now, it is observed that spatial correlation with ECMWF remains very high (85 to 95 %) and is constant throughout the whole year but DMET produces globally lower estimates than ECMWF especially in Africa and South America.

Due to limited validation in dry/(very dry) conditions (mainly in Africa regions), care should be taken when using the product for those areas (see conclusions of validation report, annex C). In its current state, evapotranspiration products can be used in the following applications:

- Regional ET estimation, in areas where no measurements are available
- Environmental monitoring purposes
- Assimilation in hydrological and crop growth models
- Long-term studies on evapotranspiration evolution related to climate.

# 6 References

Chehbouni, A., Lo Seen, D. , Njoku, E.G. and Monteny, B. 1996a. A Coupled Hydrological and Ecological modeling Approach to examine the Relationship between Radiative and Aerodynamic Surface Temperature over Sparsely Vegetated Surfaces. Remote Sensing Environment.

Choudhury, B. J., 1991: Multispectral satellite data in the context of land surface heat balance. *Rev. Geophys.*, **29,** 217–236.

Dickinson R.E., 1983: Land surface processes and climate – Surface albedos and energy balance, *Adv. Geophys.*, **25**, 305-353.

Ferranti, L. and P. Viterbo, 2006: The European Summer of 2003: Sensitivity of Soil Water Initial Conditions. *J. Climate*, **19**, 3659-3680.

Gellens-Meulenberghs, F., Arboleda, A. and Ghilain, N. 2006. Status of development of the LSA-SAF evapotranspiration product. Proc. 2nd LSA-SAF Training Workshop, Lisbon, 8-10 March, 10 pp.

Gellens-Meulenberghs, F., Arboleda, A. and Ghilain, N., 2007. Towards a continuous monitoring of evapotranspiration based on MSG data. Accepted contribution to the Proc. symposium on Remote Sensing for Environmental Monitoring and Change Detection. IAHS series. IUGG, Perugia, Italy, July 2007, 7 pp.

Masson, V., Champeaux, J. L., Chauvin, F., Meriguet, Ch. and Lacaze, R. A., 2003. Global Database of Land Surface Parameters at 1-km Resolution in Meteorological and Climate Models. J. Climate 16(9), 1261-1282.

Mitchell, K., et al., 2004: The multi-institution North American Land Data Assimilation System NLDAS: Utilizing multiple GCIP products and partners in a continental distributed hydrological modeling system, *J. Geophys. Res*., **109**, doi:10.1029/2003JD003823.

Mucher, C. A. 2000. Development of a consistent methodology to derive land cover information on a European scale from remote sensing for environmental modelling. Final Report, European Commission, DG XII."

Rodell M., P. R. Houser, U. Jambor, J. Gottschalck, K. Mitchell, C.-J. Meng, K. Arsenault, B. Cosgrove, J. Radakovich, M. Bosilovich, J. K. Entin, J. P. Walker, D. Lohmann, and D. Toll, The Global Land Data Assimilation System, 2004a: Bull. Amer. Meteor. Soc. 85(3).

Schmetz, J., P. Pili, S. Tjemkes, D. Just, J. Kerkman, S. Rota, and A. Ratier (2002), An introduction to Meteosat Second Generation (MSG), *Bull. Amer. Meteor. Soc*., *83*, 977-992.

Taylor, K.E.: Summarizing multiple aspects of model performance in a single diagram. J. Geophys. Res., 106, 7183-7192, 2001 (also see PCMDI Report 55, http://www-pcmdi.llnl.gov/publications/ab55.html).

Trigo, I. F., C. C. DaCamara, P. Viterbo, J.-L. Roujean, F. Olesen, C. Barroso, F. Camacho-de-Coca, D. Carrer, S. C. Freitas, J. García-Haro, B. Geiger, F. Gellens-Meulenberghs, N. Ghilain, J. Meliá, L. Pessanha, N. Siljamo, A Arboleda (2010), The Satellite Application Facility on Land Surface Analysis, *Int. J. Remote Sens*., in press.

van den Hurk, B., Viterbo, P., Beljaars, A. and Betts, A., 2000. Offline validation of the ERA40 surface scheme. ECMWF Techn. Memorandum No.295, 42 pp.

Viterbo, P. and Beljaars, A., 1995. An improved surface parametrization scheme in the ECMWF model and its validation. J. Climate 8, 2716-2748.

## 7 Developers

The development and implementation of the method is carried out by the Royal Meteorological Institute of Belgium (RMI)

Coordinator: Françoise Gellens-Meulenberghs

Developers: Alirio Arboleda
Nicolas Ghilain

**Glossary**

| | |
|---|---|
| AATSR: | Advanced Along Track Scanning Radiometer |
| ARM: | NASA Atmospheric Radiation Measurements Program |
| ASTER: | Advanced Spaceborne Thermal Emission and Reflection Radiometer |
| AVHRR: | Advanced Very High Resolution Radiometer |
| cwv: | column water vapour |
| ECMWF: | European Centre for Medium-Range Weather Forecasts |
| EM: | Land Surface Emissivity |
| EMAC: | European Multi-sensor Airborne Campaign |
| ENVISAT | Environmental Satellite |
| EOS: | Earth Observing System |
| EPS: | EUMETSAT Polar System |
| ESA: | European Space Agency |
| EUMETSAT: | European Meteorological Satellite Organisation |
| FIFE: | First ISLSCP Field Experiment |
| FOV | Field of View |
| FZK-IMK: | Forschungszentrum Karlsruhe – Insitut für Meteorologie und Klimaforschung (Germany) |
| GOES: | Geostationary Operational Environmental Satellite |
| GSW: | Generalized Split-Window |
| HAPEX: | Hydrological and Atmospheric Pilot Experiment in the Sahel |
| HDF | Hierarchical Data Format |
| HIRLAM: | High Resolution Limited Area Model |
| HIRS: | High Resolution Infrared Radiation Sounder |
| ICAT: | Instituto de Ciência Aplicada e Tecnologia (Portugal) |
| IM: | Instituto de Meteorologia (Portugal) |
| IPMA: | Instituto Português do Mar e da Atmosfera |
| IR: | Infrared Radiation |
| ISLSCP: | International Satellite Land Surface Climatology Project |
| LST: | Land Surface Temperature |
| LUT: | Look-Up Table |
| MAS: | Modis Airborne Simulator |
| METEOSAT: | Geostationary Meteorological Satellite |

| | |
|---|---|
| MODIS: | Moderate-Resolution Imaging Spectro-Radiometer |
| MODTRAN: | Moderate Resolution Transmittance Code |
| MSG: | Meteosat Second Generation |
| NASA: | National Air and Space Administration |
| NDVI: | Normalised Difference Vegetation Index |
| NEΔT: | Noise Equivalent Temperature |
| NIR | Near Infrared Radiation |
| NOAA: | National Oceanic and Atmospheric Administration (USA) |
| NWC: | NoWCasting SAF |
| NWP: | Numerical Weather Prediction |
| PRISM: | Process Research by Imaging Space Mission |
| QC: | Quality Control |
| rms: | root mean square |
| RSS: | Root Sum Square |
| SAF: | Satellite Application Facility |
| SEVIRI: | Spinning Enhanced Visible and InfraRed Imager |
| SPOT | Système Probatoire d'Observation de la Terre |
| SST: | Sea Surface Temperature |
| SURFRAD: | Surface Radiation Budget Network |
| TCWV: | Total Column Water Vapour |
| TIGR: | TOVS Initial Guess Retrieval |
| TIR: | Thermal Infrared |
| TIROS: | Television and Infrared Observation Satellite |
| TISI: | Temperature Independent Spectral Index |
| TOVS: | TIROS-N Operational Vertical Sounder |
| TSP: | Thermal Surface Parameter |
| TTM: | Two-Temperature Method |
| U-MARF | Unified Meteorological Archiving and Retrieval Facility |
| URD: | User Requirements Document |
| v-a: | viewing angle |
| VCM: | Vegetation Cover Method |
| VIS | Visible Radiation |

## ANNEX A –Product Output Format for LSA-SAF MET v4.0

Description of the following attributes is given in the Product Output Format Document

General attributes

| Attribute | Allowed Values |
|---|---|
| SAF | "LSA" |
| CENTRE | "IM-PT" |
| ARCHIVE_FACILITY | "IM-PT" |
| PRODUCT | "ET" |

| Attribute | Allowed Values |
|---|---|
| PARENT_PRODUCT_NAME | “DSSF”,”DSLF”,”ALB/LAI”,”SM/EM” |
| SPECTRAL_CHANNEL_ID | 0 |
| PRODUCT_ALGORITHM_VERSION | “4.0.7” |
| CLOUD_COVERAGE | “NWC-CMa” |
| OVERALL_QUALITY_FLAG | “OK” |
| ASSOCIATED_QUALITY_INFORMATION | “-“ |
| REGION_NAME | One of: “MGS-Disk”, “Euro”, “Nafr”, “SAfr”, “SAme” |
| COMPRESSION | 0 |
| FIELD_TYPE | “Product” |
| FORECAST_STEP | 0 |
| NC | One of: 1701,2211,1211,701 |
| NL | One of: 651,1151,1191,1511 |
| NB_PARAMETERS | 2 |
| NOMINAL PRODUCT_TIME | YYMMDDhhmmss |
| SATELLITE | “MSG2” |
| SATELLITE_ID | “SEVI” |
| INSTRUMENT_MODE | “STATIC_VIEW” |
| IMAGE_ACQUISITION_TIME | YYMMDDhhmmss |
| ORBIT_TYPE | ”GEO” |
| PROJECTION_NAME | « Geos<000.0> » |
| NOMINAL_LONG | -10.0 |
| NOMINAL_LAT | 0.0 |
| CFAC | 781651432 |
| LFAC | -781651432 |
| COFF | 1856 |
| LOFF | 1856 |
| PIXEL_SIZE | “3.1Km” |
| GRANULE_TYPE | “DP” |
| PROCESSING_LEVEL | “04” |
| PRODUCT_TYPE | “LSAET” |
| PROCESSING_MODE | “N” |

| Attribute | Allowed Values |
|---|---|
| MEAN_SSLAT | 1234. |
| MEAN_SSLON | 4321. |
| DISPOSITION_FLAG | “O” |
| TIME_RANGE | “30-min” |
| STATISTIC_TYPE | “N/A” |

Dataset attributes

| Attribute | Value (Product) | Value (Quality Flag) |
|---|---|---|
| CLASS | “Data” | “ET_Q_Flag” |
| PRODUCT | “ET” | “Data” |
| PRODUCT_ID | 232 | 232 |
| N_ COLS | One of: 1701,2211,1211,701 | One of: 1701,2211,1211,701 |
| N_ LINES | One of: 651,1151,1191,1511 | One of: 651,1151,1191,1511 |
| NB_BYTES | 2 | 2 |
| SCALING_FACTOR | 10000. | 1. |
| OFFSET | 0. | 0. |
| MISS_VALUE | -1 | -1 |
| UNITS | “SI” | “SI” |
| CAL_SLOPE | 999. | 999. |
| CAL_OFFSET | 999. | 999. |

YY - Year; MM-Month; DD – Day; hh – Hour; mm – Minute; ss – Second

## ANNEX B – Quality Control Information

| Bit | Field | Category | Binary code | Description |
|---|---|---|---|---|
| 00-00 | Land/Sea | Sea | 0 | |
| | | Land | 1 | |
| 01-01 | Land cover | | | |
| | | | 0 | IGBP |
| | | | 1 | ECOCLIMAP |
| 02-02 | Cloud cover | | | |
| | | | 0 | Covered |
| | | | 1 | Clear / partially covered |
| 03-04 | Snow cover | | | |
| | | | 00 | Not processed |
| | | | 01 | Snow covered |
| | | | 10 | Partially covered |
| | | | 11 | Snow-free |
| 05-06 | SM | | | |
| | | | 00 | Corrupted / not processed |
| | | | 01 | SM from LSAF-SAF |
| | | | 10 | SM from other source (ECMWF) |
| 07-07 | AL | | | |
| | | | 0 | Albedo from data base |
| | | | 1 | Albedo from AL product |
| 08-09 | LST | | | |
| | | | 00 | Not used by now |
| | | | 00 | |
| | | | 00 | |
| 10-11 | DLSF | | | |
| | | | 00 | Corrupted / not processed |
| | | | 01 | Below nominal |
| | | | 10 | Nominal |
| | | | 11 | Above nominal |
| 12-13 | DSSF | | | |
| | | | 00 | Corrupted / not processed |
| | | | 01 | Below specified angle of view |
| | | | 10 | Cloudy sky method |
| | | | 11 | Clear sky method |
| 14-15 | ET confidence | | | |
| | | | 00 | Corrupted / not processed |
| | | | 01 | Poor quality |
| | | | 10 | Below nominal |
| | | | 11 | Nominal |

**ANNEX C – Conclusions from validation report**

The validation of LSA-16 (MET) and LSA-17 (DMET) products was achieved by comparing the algorithm output (instantaneous and cumulated evapotranspiration) to evapotranspiration derived from measurements made at selected locations and by comparing the algorithm output to the output of models recognized to produce valuable meteorological information. Output from ECMWF model and GLDAS was used for the models inter-comparison. Table 1, summarizes the results of the in-situ validation, providing statistical indicators of the comparisons and percentage of cases where PRD criterion is satisfied. Points 1 to 6 resume the main conclusions of the validation report.

| Station | Vegetation Type * | Bias | RMS | Corr | % PRD |
|---|---|---|---|---|---|
| Amplero | G | 0.02 | 0.11 | 0.82 | 75.1 |
| Buzenol | G | 0.02 | 0.10 | 0.81 | 80.1 |
| Cabauw | G | 0.02 | 0.07 | 0.90 | 90.1 |
| Humain | G | -0.04 | 0.08 | 0.90 | 83.2 |
| Monte Bondone | G | 0.02 | 0.12 | 0.76 | 77.6 |
| Tojal | G | 0.05 | 0.10 | 0.74 | 59.9 |
| Hesse | DBF | 0.00 | 0.09 | 0.56 | 89.9 |
| Roccarespampani | DBF | -0.02 | 0.08 | 0.85 | 77.5 |
| Loobos | ENF | -0.03 | 0.10 | 0.63 | 86.3 |
| Wetzstein | ENF | -0.02 | 0.08 | 0.79 | 87.9 |
| Sodankylä | ENF | 0.08 | 0.12 | 0.46 | 63.8 |
| Lonzée | C | 0.03 | 0.09 | 0.73 | 73.4 |
| Las Majadas | EMF | 0.01 | 0.06 | 0.46 | 94.7 |
| Puéchabon | EMF | -0.07 | 0.09 | 0.65 | 99.7 |
| Kaamanen | B | -0.01 | 0.07 | 0.69 | 95.5 |
| Vielsalm | MF | 0.02 | 0.06 | 0.80 | 88.2 |
| Demokeya | Ss | -0.12 | 0.18 | 0.40 | 87.6 |

*Table 8. Summary of the comparison between output from MET algorithm and ET derived from measurements. Column 1 is the name of station; column 2, the vegetation type considered at station; column 3 the root mean square of the comparison; column 4 the correlation coefficient; column 5 the bias ; column 6 the percentage of steps for which PRD requirements are met.*
** Grassland (G), Deciduous Broadleaved Forest (DBF), Evergreen Needle Forest (ENF), Crops (C), Mixed Forest (MF), Evergreen Mediterranean Forest (EMF), Ss (Sahelian savannah)*

1) Results of the in-situ validation summarized in table 8 show that for estimates flagged 'Nominal' or 'Below Nominal', the PRD quality criterion is satisfied to a rate higher than 70%. Globally, good agreement is found for stations at which close correspondence exist between land cover defined in ECOCLIMAP and the effective cover at the station; with the best agreement for stations over grassland and mixed forests. The model does not present systematic bias; nevertheless modelled ET is underestimated at a station (Demokeya) over African dry savannah. In general, LSA-SAF MET algorithm is able to reproduce the temporal evolution of evapotranspiration with values equivalent to observations.

2) From the models inter-comparison, it is concluded that ET estimates provided by the MET algorithm are equivalent to estimates provided by ECMWF and GLDAS, with spatial correlation between 85% and 95% for midday images. For high co-zenithal angles better correlation is found with ECMWF while for low angles (spring/late autumn and morning/evening) with GLDAS. Observed discrepancies between models estimates are explained by differences in models parameterization, radiation, land cover information and soil water content.

3) From the consistency check it is observed that uncertainties on AL, DSSF and DSLF used as input to MET are correctly reflected on MET quality flag. The comparison of morning heating rates from Tskin and LST highlighted regions of low /high correlations which correspond roughly to areas of large relative bias between MET and GLDAS ET. Given that relationships between FVC and LST/Tskin can provide some insight to soil water content, regions of low correlation indicate that there is still place for improvements related to soil moisture and/or vegetation parameterization.

4) For the validations of the daily product, the output of the DMET algorithm has been compared to daily-cumulated ET values at selected locations. Overall, DMET fairly matches the observed variations, with a very good agreement with observations for well-watered sites and a good seasonal variation for temperate forests.

5) The comparisons of DMET product to ECMWF daily-accumulated ET for December 2009, over the four windows defined inside the MSG FOV, confirm the results obtained during the validation of instantaneous product. I.e., the spatial correlation between the models estimates is high (85% to 95%) and remains quite constant during the analysed period.

6) The validation of the instantaneous and daily products (in-situ and models inter-comparison) provides higher scores for comparisons over Europe. For Africa and South America, the work must be continued in order to check and/or improve the quality of modelled estimations over areas affected by strong soil water stress. Further improvements of the MET algorithm will have positive impact on both MET and DMET products.